Isı Bilimi ve Tekniği Dergisi, 36, 2, 41-49, 2016
J. of Thermal Science and Technology

ISSN 1300-3615

A COMPARISON OF AN ANALYTICAL AND NUMERICAL FLOW MODEL FOR THE LUBRICATION SYSTEM OF A VARIABLE SPEED HERMETIC COMPRESSOR

Mustafa OZSIPAHI*, Sertac CADIRCI, Hasan GUNES*** and Kemal SARIOGLU******
Department of Mechanical Engineering, Istanbul Technical University, 34437 Gumussuyu, Istanbul
Arcelik Research and Development Center, 34950 Tuzla, Istanbul
*ozsipahimu@itu.edu.tr, **cadircis@itu.edu.tr, ***guneshasa@itu.edu.tr, ****kemal.sarioglu@arcelik.com

(Geliş Tarihi: 20.02.2015, Kabul Tarihi: 09.05.2016)

Abstract: This study presents an analytical flow model for the screw pump and compares it with the numerical simulations for the lubrication system of a variable speed hermetic reciprocating compressor used mainly in household refrigerators. Since variable capacity compressors (VCC) can be operated at different rotational speeds, a sufficient lubrication is required even at low rotational speeds where centrifugal effects are at a minimum. The lubrication system of such compressors includes a screw pump inside their crankshaft for this purpose. Using the analytical flow model, effects of the main design parameters for the screw pump to maximize the mass flow rate of the lubricant released from the upper part of the crankshaft are predicted and compared with numerical results. Specifically, the effects of the rotational speed, the oil viscosity, the submersion depth of the crankshaft in the oil sump and screw aspect ratio are investigated in this paper.
Keywords: Variable capacity hermetic compressor, Lubrication, Screw pump, Analytical flow model, Computational Fluid Dynamics (CFD).

DEĞİŞKEN DEVİRLİ HERMETİK KOMPRESÖR YAĞLAMA SİSTEMİ İÇİN AKIŞ MODELİNİN ANALİTİK VE SAYISAL OLARAK KARŞILAŞTIRILMASI

Özet: Bu çalışmada ev tipi buzdolaplarında kullanılan değişken devirli hermetik pistonlu kompresörlerin yağlama sisteminde bulunan vidalı pompa etrafındaki akış analitik olarak modellenmiş olup, sayısal modellemeler ile karşılaştırılmıştır. Değişken kapasiteli kompresörler (VCC) farklı devir sayılarında çalıştırılabildikleri için, merkezkaç etkilerin en az seviyede olduğu düşük devir sayılarında dahi yeterli bir yağlamaya ihtiyaç duyulmaktadır. Bu amaç için, krank mili içerisinde yer alan vidalı pompa bu tip kompresörlerin yağlama sisteminin bir parçasıdır. Analitik akış modeli kullanılarak, krank mili ucundan çıkan kütlesel yağ debisini arttıracak ana tasarım parametrelerinin etkileri tahmin edilmiş ve sayısal sonuçlar ile karşılaştırılmıştır. Bu çalışmada özellikle devir sayısının, yağ viskozitesinin, krank milinin yağ haznesi içerindeki daldırma derinliğinin ve vida diş oranının etkileri incelenmiştir.
Anahtar Kelimeler: Değişken kapasiteli hermetik kompresör, Yağlama, Vidalı pompa, Analitik akış modeli, Hesaplamalı Akışkanlar Dinamiği (HAD).

NOMENCLATURE

b_i	coefficients of the eigenfunctions
dt	time step [s]
g	gravitational acceleration [m/s^2]
h_B	pump height [m]
h_{oil}	submersion depth [m]
H	channel depth [m]
k	dimensionless pressure drop
m	mass flow rate [kg/s]
n	rotation [rpm]
p	pressure [N/m^2]
R_B	internal radius of the crankshaft [m]
t	time [s]
u	velocity in x-direction [m/s]
v	velocity in y-direction [m/s]
w	velocity in z-direction [m/s]
W	channel width [m]

Greek symbols

α	volume fraction
β	screw helix angle
γ	screw aspect ratio [$=W/H$]
κ	screw curvature ratio [$=H/R_B$]
μ	dynamic viscosity [kg/ms]
ν	kinematic viscosity [m^2/s]
ρ	density [kg/m^3]
τ	surface tension between phases [N/m]
Ω	rotational speed [rpm]

Abbreviations

VCC	Varaible Capacity Compressor
COP	Coefficient of Performance
VoF	Volume of Fluid

INTRODUCTION

In the last decade, variable capacity compressors are started to be used with a rising tendency in order to provide energy efficient refrigeration and higher comfort for customers. Since the cooling capacity requirement according to operating conditions is achieved by changing the rotational

speed, the need of an effective lubrication at low rotational speeds intensifies the prerequisites for a new design of the oil management system. The coefficient of performance (COP) of a compressor directly affects the cooling unit energy consumption. Mechanical efficiency is one of the crucial parameters that has an impact on the COP of the compressor. Therefore, the lubrication system in a reciprocating compressor is not only vital for providing expected lifetime of the compressor but also for keeping the desired performance of the compressor at various operating conditions.

An important difference in the design of constant and variable speed compressors which comes into prominence is that the constant speed compressor delivers the lubricant through an eccentric and inclined channel through the crankshaft while the other one usually possesses a *screw pump* located concentrically inside the axisymmetric channel of the crankshaft which has potential to deliver the lubricant even at low rotational speeds.

Lückmann et al. (2008, 2009) investigated oil pumping in a reciprocating compressor and carried out numerical studies to reveal the climbing time of the oil film. Two-phase flow is simulated using the volume of fluid (VoF) method and the numerical results have been reported to be in good agreement with the experimental results. The oil climbing time is found to be 0.6 seconds and it is shown that even minor simplifications such as neglecting the radial clearance region between the shaft bearings; can affect the oil flow rate significantly.

Kerpicci et al. (2010) modeled oil flow in a hermetic reciprocating compressor designed for constant speed (eccentric hole without screw pump) and reported the effects of the rotational speed and viscosity on the mass flow rates. It is shown that for rotational speeds varying between 3000 and 5000 rpm, the mass flow rate is almost doubled. Another important finding is that with increasing viscosity, the mass flow rate decreases significantly.

Alves et al. (2012, 2013) used a semi-analytical technique to reveal the effects of the geometric parameters on the oil flow rates in an eccentric tube centrifugal oil pumping system for hermetic compressors. It is found that the volumetric flow rate was increased with the pick-up tube diameter and shaft eccentricity, as larger diameters generate less friction and larger eccentricities induce a higher centrifugal acceleration. However the effect of the shaft eccentricity is found to be more pronounced.

Alves et al. (2011) developed an analytical solution for fluid flow in a screw pump oil supply system for reciprocating compressors. The Poisson equation with boundary conditions for the screw pump region is solved analytically and the flow rate is calculated from the velocity distribution. The pressure gradient is defined as a function of the submersion depth of the crank shaft in the oil sump and screw helix angle. The constant in the Poisson equation is parameterized for both the screw pump and shaft channel regions. It is shown that varying the rotational speeds between 500 and 2000 rpm has significant effect on the oil flow rates.

Wu et al. (2010) analyzed oil pumping in a hermetic reciprocating compressor for household refrigerators. They focused on the centrifugal forces on the oil pumping and it was shown that the existing design of the reed pump would fail to deliver oil when the rotational speed was below 2000 rpm.

Kim et al. (2002) simulated an oil supply system of a reciprocating compressor for household refrigerators and presented analytical solutions for oil flow rates to the spiral groove, journal bearing and thrust bearing. It was found that with increasing viscosity the flow rates decreased especially for higher rotational speeds as high as 3600 rpm. On the other hand, the effects of the geometric parameters such as the groove area and the groove angle are presented. When both parameters are increased, the oil flow rate also increases.

Li and Hsieh (1996) obtained an analytical solution of an isothermal, Newtonian flow in a single screw extruder with a finite channel. They simplified the Navier-Stokes equation in flow direction to a Poisson equation and specified boundary conditions for the barrel, screw root and screw flights. They applied finite sine-transformation method to this second order partial differential equation with non-homogeneous boundary conditions. The velocity profiles are presented in three dimensional plots to reveal the effect of the screw flights.

Alves et al. (2009) developed an analytical solution of single screw extrusion which is applicable to intermediate values of screw channel aspect ratio. Generalized integral transform technique (GITT) which is flexible with respect to nature of the non-homogeneities in the partial differential equation and boundary conditions is utilized to obtain the analytical solution of the velocity distribution. For various screw aspect ratios and screw curvature ratios, the effect of the helix ratio on the flow rates could be investigated.

Ozsipahi et al. (2014) modeled the lubrication system for a constant capacity hermetic reciprocating compressor using a laminar, incompressible and transient flow solver and obtained mass flow rates for various operating conditions. Using the VoF method to simulate the two phase flow for the lubricant and refrigerant, it is found that with increasing rotational speed, submersion depths and decreasing oil viscosity, the mass flow rates increase.

Ozsipahi et al. (2014) investigated the effects of main geometric parameters on the lubrication system of a constant capacity hermetic reciprocating compressor. It was shown that the cross-sectional area of the helical channel plays an important role in increasing the mass flow rates. For example, deepening the helical channel plays a more significant role in increasing the mass flow rate rather than extending and changing other geometric parameters.

Tada et al. (2014) used an uncoupled simulation model and carried out experiments for the oil pumping system of a variable capacity compressor. The experiments revealed that for a constant rotational speed, the average flow rate increases slightly with increasing immersion depth of the crankshaft.

In this paper, an analytical flow model for the screw pump is obtained and validated with full CFD simulations to

investigate the effects of physical and geometric parameters which may change the mass flow rates released from the crankshaft outlet. This study includes the effects of the rotational speed of the crankshaft, oil viscosity, submersion depth of the crankshaft in the oil sump and screw pump geometric parameters. The geometry used in this study is shown in Fig.1. The lubricant which is sucked through the suction hole on the bottom surface of the crankshaft flows in the screw pump and reaches the crank lower bearings. Then, it is directed to the helical channel which is carved on the external surface of the crankshaft and lubricates crank upper bearings. Finally, the lubricant flows to the outlet of the crankshaft to lubricate the piston-cylinder group and the juncture between the piston and the crankshaft and returns to the oil sump.

The paper is organized as follows: in Section 2, the CFD modeling approach and computational aspects are presented in detail. Section 3 includes the analytical approach with the simplified problem formulation and the analytical solution in a closed form. In Section 4, the results from numerical modeling and analytical solution are presented for various physical and geometric parameters. Finally in Section 5 main findings are discussed.

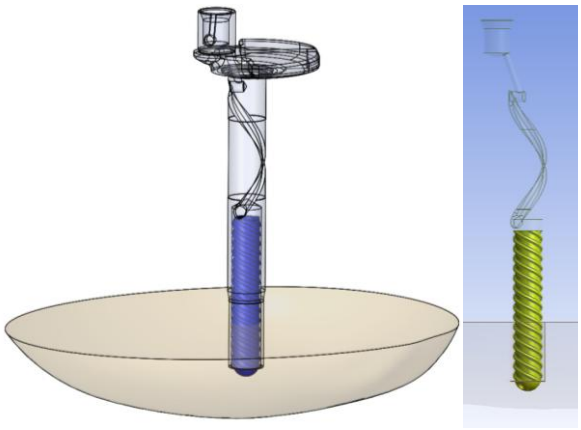

Figure 1. Detailed appearance of the crankshaft and the screw pump of the variable speed hermetic reciprocating compressor

CFD MODELING

Computational Domain and Boundary Conditions

Two distinct models were investigated numerically. In Case (A), the lubrication system is divided into two parts, namely: the smooth crankshaft prescribed with rotating-wall including a stationary screw pump. In Case (B), the crankshaft with screw flights on its internal surface prescribed with rotating-wall and a stationary smooth cylindrical apparatus inside the crankshaft. In both cases the oil sump is stationary.

To obtain reliable numerical results and sufficient discretization, calculations have been performed with three different dense meshes using a time step of dt = 10-4 seconds and the mass flow rates are tabulated in Table 1. The unsteady analysis was performed for a rotational speed of 3000 rpm, an oil viscosity of 5 cSt and submersion depth of 20 mm and a screw aspect ratio of 2.04. Mass flow rates shown in Table 1 were obtained after a computational time of at least 5 seconds.

Table 1 indicates that a computational domain consisting of nearly 380000 polyhedral elements was found to be sufficiently dense to obtain consistent solutions. A typical mesh is shown in Fig.2 where grid refinement was performed close to solid walls and interfaces between adjacent domains.

As Table 1 shows, a time step of $dt = 10^{-4}$ seconds was considered to be sufficient as there was no considerable change in the mass flow rates with further decreasing time step after steady state flow conditions are achieved.

Table 1. Grid independence and time resolution tests

Number of cells	$m_{Numerical}$ [g/s]	Time step [s]	$m_{Numerical}$ [g/s]
285000	2.2	5e-05	2.3
380000	2.3	1e-04	2.3
565000	2.3	1.5e-4	2.2

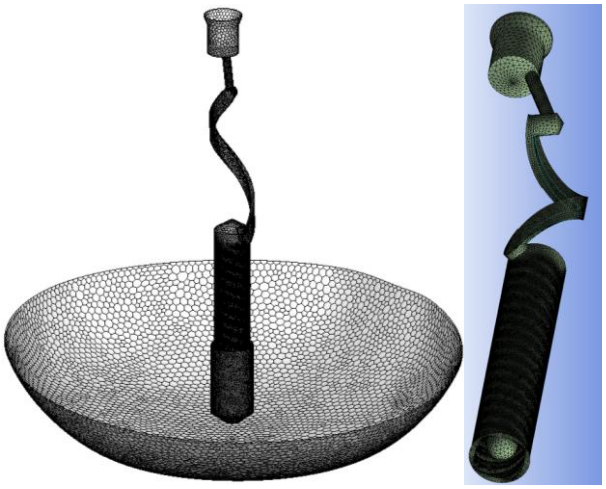

Figure 2. Computational domain for the lubrication system for Case (A).

In the simulations oil was elevated to the crankshaft outlet and did not return to the oil sump. The boundary conditions for the mass and momentum equations were specified as follows: (i) prescribed pressure at the top of the free surface in the oil sump and crankshaft outlet, as both surfaces were imposed to the same pressure; (ii) angular velocity of the crankshaft walls was set equal to the speed of the electrical motor rotor neglecting its acceleration, (iii) all remaining walls for both cases and interfaces between domains were stationary.

Computational Aspects

The fluid flow in the oil supply system was solved numerically using the finite-volume based ANSYS-Fluent package with the following assumptions: (i) since under compressor operating condition of 0.624 bar and 70°C, the refrigerant is dissolved only approximately 2% in oil, the mixture is assumed to be immiscible, (ii) the flow is isothermal, (iii) the physical properties of the fluids (oil and refrigerant) are constant, (iv) the gaseous refrigerant is replaced by air as the thermo-physical properties of air are

very close to those of the gaseous refrigerant (iso-butane with a density of 1.27 kg/m^3 at 0.624 bar and 70°C and dynamic viscosity of 8.72 x 10^{-6} kg/ms).

The conditions of the numerical simulation are as follows: (i) rotational speed (Ω) is 1000, 2100 and 3000 rpm; (ii) the depth of the crankshaft submerged in the oil sump (h_{oil}) is 10, 15 and 20 mm, (iii) the working pressure is actually 0.624 bar, but the pressure difference between the crankshaft exit and the oil sump is set equal to zero; (iv) refrigerant is replaced with air with a density of 1.23 kg/m^3 and a viscosity of 1.5 x 10^{-5} kg/ms; (v) the lubrication oil with a density of (ρ) 890 kg/m^3, the kinematic viscosity of oil (ν) is 3,5, 10 or 15 cSt and (vi) surface tension (τ) between the phases is 0.024 N/m.

Parallel computations have been performed on a 12-core processor computer using a second-order upwind scheme with appropriately selected underrelaxation factors for discretizing the continuity and momentum equations and the VoF model is used for phase tracking. Implicit PISO (Pressure-Implicit with Splitting Operators) algorithm is used for pressure-velocity coupling since it handles well the small time steps. The convergence criteria for the continuity, momentum and VoF equations are set to 10^{-4} RMS.

Governing Equations

The climbing time, the oil flow distribution to the bearings and the mass flow rate of the lubricant play a significant role in an effective lubrication system. Mass flow rate based Reynolds number for investigated flow domain is around 70, therefore a two phase, isothermal, laminar and incompressible flow model with Volume of Fluid (VoF) approximation is selected in the flow solver. For a two-phase flow, the continuity equation including the volume fractions (α_l) is given in Eq. (1) where *l* denotes the liquid phase (Ansys, 2014).

$$\frac{\partial}{\partial t}\left(\alpha_l \rho_l\right)+\nabla\left(\alpha_l \rho_l \vec{u}_l\right)=0 \qquad (1)$$

The momentum equations for both phases are given in Eq. (2).

$$\rho\left[\frac{\partial \vec{u}}{\partial t}+\nabla\left(\vec{u}\vec{u}\right)\right]=\rho\vec{g}-\nabla p+\nabla\left[\mu\left(\nabla\vec{u}+\nabla\vec{u}^{T}\right)\right] \qquad (2)$$

ANALYTICAL APPROACH

Problem Formulation and Boundary Conditions

A simplified analytical model is derived based on the vanishing inertia terms for viscosity dominated flows and resulting in Poisson's equation which is solved analytically using an integral transform technique. In the analytical approach, the screw curvature (H/R_b) is assumed to be small and the curved surfaces of the channel can be *unwrapped* to become flat plates as denoted by *Li and Hsieh* (1996) and *Alves et al.* (2009). The momentum equations given in Eq. (2) for steady and laminar Newtonian, isothermal and incompressible flow are written in Eq. (3). The effect of gravity in the momentum equations is ignored; however, it is imposed as submersion depth based on hydrostatic pressure in the definition of the dimensionless pressure gradient.

$$\begin{aligned}
\rho\left(u\frac{\partial u}{\partial x}+v\frac{\partial u}{\partial y}+w\frac{\partial u}{\partial z}\right)&=-\frac{\partial p}{\partial x}+\mu\left(\frac{\partial^2 u}{\partial x^2}+\frac{\partial^2 u}{\partial y^2}+\frac{\partial^2 u}{\partial z^2}\right)\\
\rho\left(u\frac{\partial v}{\partial x}+v\frac{\partial v}{\partial y}+w\frac{\partial v}{\partial z}\right)&=-\frac{\partial p}{\partial y}+\mu\left(\frac{\partial^2 v}{\partial x^2}+\frac{\partial^2 v}{\partial y^2}+\frac{\partial^2 v}{\partial z^2}\right)\\
\rho\left(u\frac{\partial w}{\partial x}+v\frac{\partial w}{\partial y}+w\frac{\partial w}{\partial z}\right)&=-\frac{\partial p}{\partial z}+\mu\left(\frac{\partial^2 w}{\partial x^2}+\frac{\partial^2 w}{\partial y^2}+\frac{\partial^2 w}{\partial z^2}\right)
\end{aligned} \qquad (3)$$

Equation (3) can be simplified since the inertia forces are negligible due to low velocities of the lubricant and the characteristic dimensions of the problem are small (i.e., low Reynolds number). Assuming no flow in *y*-direction, the Navier-Stokes equations can be rewritten for a fully developed flow as in Eq. (4).

$$\begin{aligned}
&\frac{1}{\mu}\frac{\partial p}{\partial x}\approx\frac{\partial^2 u}{\partial y^2}\\
&\frac{\partial p}{\partial y}\approx 0\\
&\frac{1}{\mu}\frac{\partial p}{\partial z}=\frac{\partial^2 w}{\partial x^2}+\frac{\partial^2 w}{\partial y^2}
\end{aligned} \qquad (4)$$

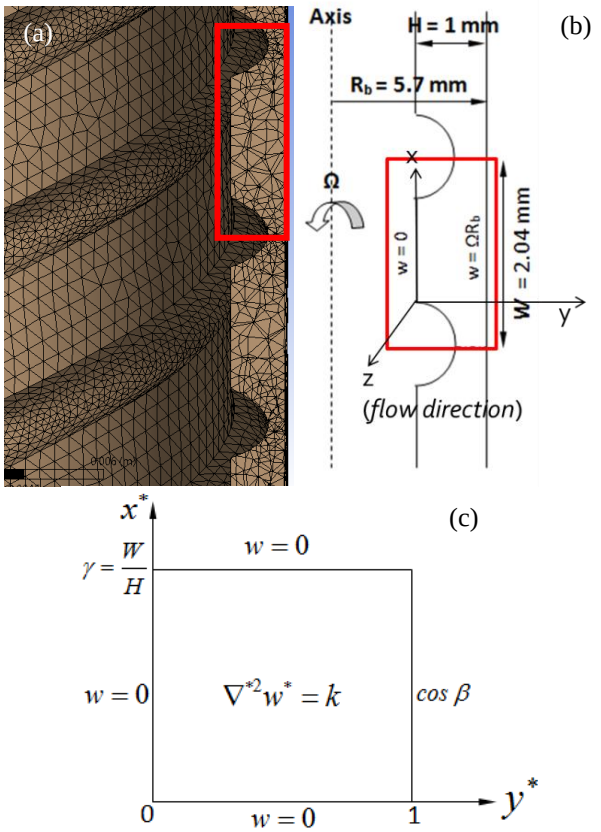

Figure 3. Domain for the analytical solution of Case (A): (a) mesh, (b) schematic view of the flow domain and (c) simplified geometry of the flow domain with boundary conditions

Figure 3 shows the coordinate system and main screw parameters for Case (A). The dimensionless variables were

obtained by normalizing x and y by the channel depth (H) and the z-velocity component w was normalized by ΩR_B where R_B denotes the internal radius of the crankshaft. The non-dimensional boundary conditions considered for Case (A) are given in Eq. (5) where β denotes the screw helix angle. Screw aspect ratio is denoted by γ. Case (A) is the basic model for the lubrication system of the variable speed compressor.

$$\begin{aligned} w^*\left(x^*,0\right)&=0\\ w^*\left(x^*,1\right)&=\cos\beta\\ w\left(0,y^*\right)&=0\\ w^*\left(\gamma,y^*\right)&=0 \end{aligned} \tag{5}$$

The Poisson equation in Eq. (4) is given in non-dimensional form in Eq. (6) where the constant pressure gradient takes the form of k. The screw helix angle changes with the screw pitch (Λ) since it relates to $\Lambda = 2\pi R_B \tan\beta$. In Eq. (6), h_B denotes the total pumping head.

$$\frac{\partial^2 w^*}{\partial x^{*2}}+\frac{\partial^2 w^*}{\partial y^{*2}}=\frac{\rho g H^2 \sin\beta}{\mu\Omega R_B}\left(1-\frac{h_{oil}}{h_B}\right)=k \tag{6}$$

Problem Formulation and Boundary Conditions for Case (B)

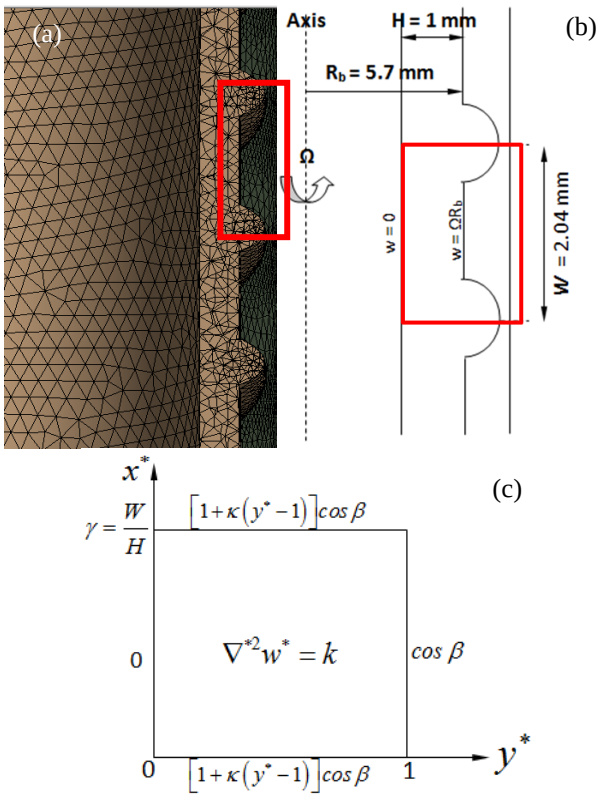

Figure 4. Domain for the analytical solution of Case (A): (a) mesh, (b) schematic view of the flow domain and (c) simplified geometry of the flow domain with boundary conditions

The non-dimensional boundary conditions for Case (B) are given in Eq. (7) where κ stands for the screw curvature ratio (H/R_B). Case (B) is an alternative model for the lubrication system of the variable speed compressor which is found to be capable of increasing the mass flow rates considerably.

$$\begin{aligned} w^*\left(x^*,0\right)&=0\\ w^*\left(x^*,1\right)&=\cos\beta\\ w\left(0,y^*\right)&=\left[1+\kappa\left(y^*-1\right)\right]\cos\beta\\ w^*\left(\gamma,y^*\right)&=\left[1+\kappa\left(y^*-1\right)\right]\cos\beta \end{aligned} \tag{7}$$

Introducing the following change of variables in Eq. (8);

$$\vartheta\left(x^*,y^*\right)=w^*\left(x^*,y^*\right)-\left[1+\kappa\left(y^*-1\right)\right]\cos\beta \tag{8}$$

boundary conditions given Eq. (7) can be written as in Eq. (9) and in turn the Poisson equation in Eq. (6) takes the form given in Eq. (10).

$$\begin{aligned} \vartheta\left(x^*,0\right)&=\left(\kappa-1\right)\cos\beta\\ \vartheta\left(x^*,1\right)&=0\\ \vartheta\left(0,y^*\right)&=0\\ \vartheta\left(\gamma,y^*\right)&=0 \end{aligned} \tag{9}$$

$$\frac{\partial^2\vartheta}{\partial x^{*2}}+\frac{\partial^2\vartheta}{\partial y^{*2}}=k \tag{10}$$

Mathematical Solution

The boundary value problems for Cases (A) and (B) can be solved by various analytical methods. Since the problem is linear, it is possible to use superposition principle coupled with standard analytical methods such as separation of variables. As the method of separation of variables fails for large screw aspect ratio values (γ), the sine integral transform was used instead of it. Integral transforms are known to be more flexible with respect to the nature of the non-homogeneities in the partial differential equation and boundary conditions.

In the first step of the finite sine integral transform, the velocity (w or ϑ) was expanded in a series of the eigenfunctions given in Eq. (11). Differentiating Eq. (11) twice with respect to x^* and y^*, then substituting them into Poisson's equation, a second order ordinary differential equation (ODE) was obtained as indicated in Eq. (12).

$$w\left(x^*,y^*\right)=\sum_i^{\infty} b_i\left(y^*\right)\sin\left(\frac{i\pi x^*}{\gamma}\right) \tag{11}$$

$$\frac{d^2 b_i\left(y^*\right)}{dy^{*2}}-\left(\frac{i\pi}{\gamma}\right)^2 b_i\left(y^*\right)=\frac{1}{\mu}\frac{dp}{dz}\frac{2}{i\pi}\left[1-(-1)^i\right] \tag{12}$$

To be able to solve the ODE given in Eq. (12), the coefficients of eigenfunctions b_i must be defined. Using the finite sine integral transformation of the velocity function, b_i can be obtained in Eq. (13). Due to the orthogonality, the right hand side of Eq. (13a) becomes $\gamma/2$ and the coefficients of the eigenfunctions can be obtained from Eq. (13b). Note

that the boundary conditions for Case (A) are $b_i(y^*=0) = 0$ and $b_i(y^*=1) = \cos\beta$.

$$\int_0^{\gamma} w(x^*,y^*)\sin\left(\frac{i\pi x^*}{\gamma}\right)dx^* = \sum_i^{\infty}\int_0^{\gamma} b_i(y^*)\sin\left(\frac{i\pi x^*}{\gamma}\right)\sin\left(\frac{i\pi x^*}{\gamma}\right)dx^* \quad (13a)$$

$$b_i(y^*) = \frac{2}{\gamma}\int_0^{\gamma} w(x^*,y^*)\sin\left(\frac{i\pi x^*}{\gamma}\right)dx^* \quad (13b)$$

After finding b_i, the velocity distribution in Eq. (11) takes the form as shown in Eq. (14):

$$w(x^*,y^*) = \sum_{i=1,3,5..}^{\infty}\frac{4\cos\beta}{i\pi}\frac{\sinh\left(\frac{i\pi y^*}{\gamma}\right)}{\sinh\left(\frac{i\pi}{\gamma}\right)}\sin\left(\frac{i\pi x^*}{\gamma}\right) + \\ + \frac{1}{\mu}\frac{dp}{dz}\frac{4\gamma^2}{(i\pi)^3}\left\{\frac{\sinh\left[\frac{i\pi}{\gamma}(1-y^*)\right]+\sinh\left(\frac{i\pi y^*}{\gamma}\right)}{\sinh\left(\frac{i\pi}{\gamma}\right)}-1\right\}\sin\left(\frac{i\pi x^*}{\gamma}\right) \quad (14)$$

The same mathematical procedure can be followed for Case (B). The problem only differs in the boundary conditions. For Case (B) the boundary conditions for the coefficients of the eigenfunctions are $b_i(y^*=0) = (\kappa\text{-}1)\cos\beta$ and $b_i(y^*=1) = 0$. The velocity distribution is obtained as given in Eq. (15).

$$\vartheta(x^*,y^*) = \sum_{i=1,3,5..}^{\infty}\frac{4(\kappa-1)\cos\beta}{i\pi}\frac{\sinh\left[\frac{i\pi}{\gamma}(1-y^*)\right]}{\sinh\left(\frac{i\pi}{\gamma}\right)}\sin\left(\frac{i\pi x^*}{\gamma}\right) + \\ + \frac{1}{\mu}\frac{dp}{dz}\frac{4\gamma^2}{(i\pi)^3}\left\{\frac{\sinh\left[\frac{i\pi}{\gamma}(1-y^*)\right]+\sinh\left(\frac{i\pi y^*}{\gamma}\right)}{\sinh\left(\frac{i\pi}{\gamma}\right)}-1\right\}\sin\left(\frac{i\pi x^*}{\gamma}\right) \quad (15)$$

The oil mass flow rate can be calculated by integrating the velocity field in x- and y- directions. After converting the problem back into dimensional form, the mass flow rate can be obtained as in Eq. (16):

$$m_{analytical} = \rho\Omega R_B H^2\int_0^W\int_0^H w(x,y)dydx \quad (16)$$

RESULTS

Effect of Viscosity

To investigate the effect of oil viscosity on the mass flow rates, the kinematic viscosity was changed between 3 and 15 cSt. Table 2 shows the mean mass flow rates for various viscosities obtained from the analytical solution of the Poisson equation and the numerical simulations by the flow solver ANSYS-Fluent. Since the analytical modeling was capable of solving the flow in screw pump region, the numerical mass flow rate to the lower bearing was considered. In both analytical and numerical solutions with increasing viscosity, the mass flow rates increased slightly. The flow is dominated by viscous forces and oil with high viscosity has the advance to stick on the walls of the screw pump easier than thinner oil, thus the mass flow rates have a tendency to increase slightly for the screw pump

Table 2. Mean mass flow rates for Case (A): Ω = 3000 rpm, h_{oil} = 20 mm and $\beta = 21.35^\circ$

ν [cSt]	$m_{Analytical}$ [g/s]	$m_{Numerical}$ [g/s]	Difference [%]
3	3.1	2.3	26
5	3.2	2.3	28
10	3.3	2.4	27
15	3.3	2.5	24

Effect of Submersion Depth

Table 3 indicates the variation of the mass flow rates for three different submersion depths. The submersion depth of the crankshaft in the oil sump together with the pumping head were realized as parameters in the Poisson equation, however they had no effect on the mass flow rates, since the variation of the h_{oil}/h_B ratio in the right hand side of the Poisson equation was very slight.

Table 3. Mean mass flow rates for Case (A): Ω = 3000 rpm, ν=5 cSt and $\beta = 21.35^\circ$

h_{oil} [mm]	$m_{Analytical}$ [g/s]	$m_{Numerical}$ [g/s]	Difference [%]
10	3.2	2.2	31
15	3.2	2.3	28
20	3.2	2.3	28

Effect of Rotational Speed

The rotational speed is the most significant factor influencing the mass flow rate. Table 4 indicates the variation of the mass flow rate with respect to the rotational speed. The increase in the mass flow rate due to increasing rotational speed is much more remarkable as this type of flow is a highly viscous flow and profoundly dominated by centrifugal forces.

The tendencies of the mass flow rate with increasing viscosity, submersion depth and rotational speeds were both identical in the analytical approach and the numerical simulations. Numerical simulations give, of course, a more realistic vision to depict the effects of these parameters, but they are too much time-consuming since the flow solver considers unsteady, three-dimensional Navier-Stokes equations in a complex and high-density mesh. On the other hand, the analytical model employed in this paper gives a rather reliable, but much faster prediction of the mass flow rates. In addition, the analytical model in its closed form is most helpful for commenting on the parameter variations at a blink.

Table 4. Mean mass flow rates for Case (A): ν=5 cSt, h_{oil} = 20 mm and $\beta = 21.35^\circ$

Ω [rpm]	$m_{Analytical}$ [g/s]	$m_{Numerical}$ [g/s]	Difference [%]
1000	1	0.7	30
2100	2.2	1.6	27
3000	3.2	2.3	28

Effect of Screw Aspect Ratio

Screw aspect ratio is one of the most crucial geometric parameters affecting the mass flow rate. The inner radius of the crankshaft is kept constant in this study. Increasing the screw aspect ratio increased the mass flow rate up to a certain value.

Figure 5 shows the screw pumps with various pitch lengths i.e., screw aspect ratios used in the numerical simulations. Figure 6 indicates the transient variation of the mass flow rates through the crankshaft's outlet for selected screw aspect ratios. After a computational time of approximately three seconds, the mass flow rates level off a steady-state regime which is tabulated in Table 5 in comparison with analytical results. With increasing screw aspect ratios up to a certain limit, the climbing time of oil decreases because the total oil path decreases.

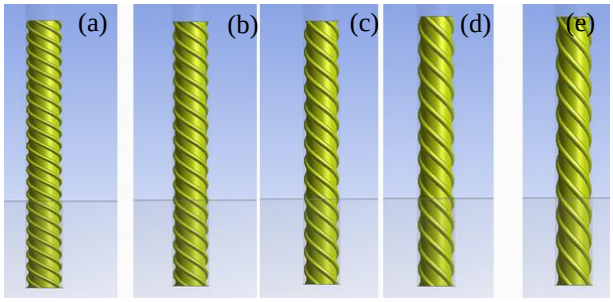

Figure 4b. Screw pumps with various screw aspect ratios: (a) γ = 2.04; (b) γ = 2.41, (c) γ = 2.77, (d) γ = 3.08 and (e) γ = 3.29

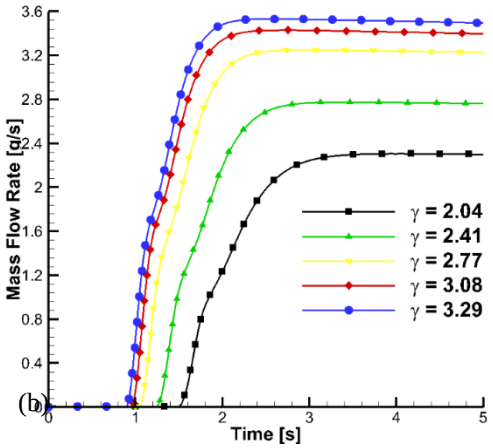

Figure 6. Mass flow rate variation with respect to time for various screw aspect ratios (numerical simulations)

Table 5. Mean mass flow rates for Case (A): ν=5 cSt, h_{oil} = 20 mm and β = 21.35°

γ	β [°]	$m_{Analytical}$ [g/s]	$m_{Numerical}$ [g/s]	Difference [%]
2.04	21.4	3.2	2.3	28
2.41	26.7	3.8	2.8	26
2.77	31.6	4.3	3.3	23
3.08	36	4.6	3.4	26
3.29	40	4.6	3.4	26

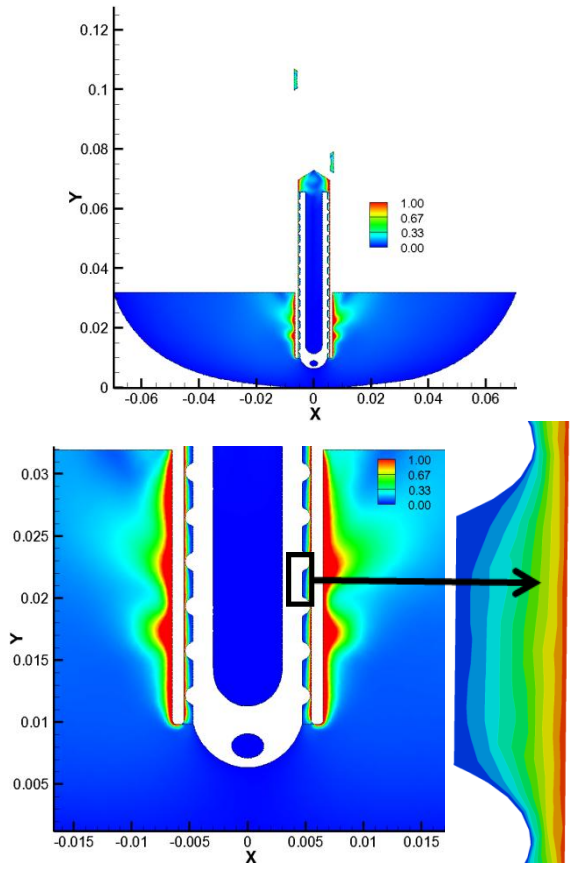

Figure 7. Velocity contours for Ω = 3000 rpm, ν = 5 cSt, h_{oil} = 20 mm and γ = 2.04 by numerical simulations.

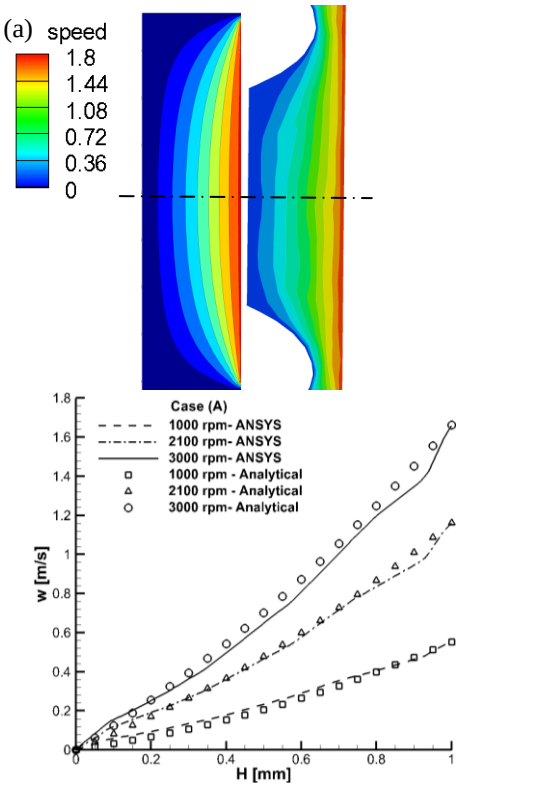

Figure 8. Case (A): (a) velocity distribution and (b) velocity profiles at the mid-section.

The flow domain of interest which was solved analytically and numerically for Case (A) is magnified in Fig. 8a and the velocity contours revealed a very similar distribution. Velocity is maximum on the boundary of rotating crankshaft and the colors denote the velocity magnitude in m/s. Fig. 8b shows velocity profiles extracted across the mid-section of the flow domain for various rotational speeds. The velocity profiles can be predicted successfully by the analytical model and a good agreement between the numerical and analytical solutions is found.

The analytically and numerically obtained velocity distribution for Case (B) can be seen in Fig.9a. The distance between the screw flight and the cylindrical apparatus in the numerical calculations was larger than the distance assumed in the analytical model. As a result, the numerical simulations give higher mass flow rates than the analytical model considerably at high rotational speeds as indicated in Table 6.

Fig. 9b shows the velocity profiles extracted across mid-section of the flow domain for various rotational speeds. The periodic boundary conditions imposed as linear velocity in Eq. (7) give rise to the velocity profiles a linear distribution compared to Case (A).

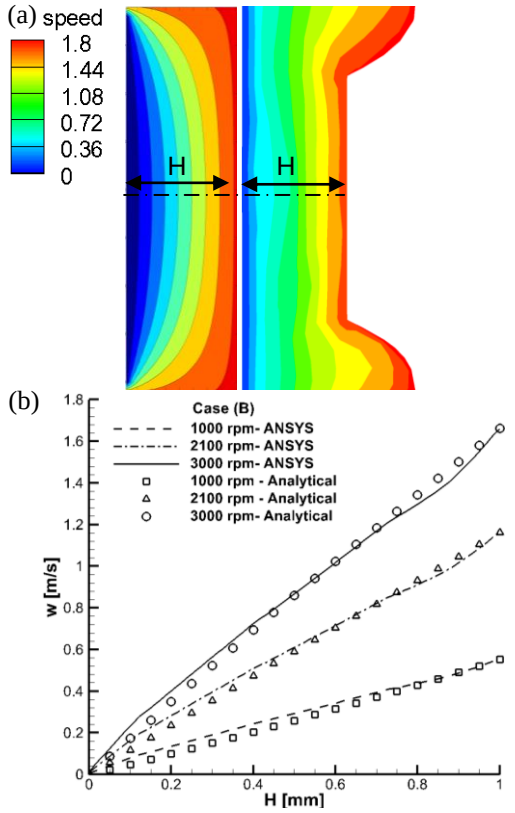

Figure 9. Case (B): (a) velocity distribution and (b) velocity profiles at the mid-section.

Table 5. Mean mass flow rates for Case (B): ν=5 cSt, h_{oil} = 20 mm and $\beta = 21.35^{\circ}$

Ω [rpm]	$m_{Analytical}$ [g/s]	$m_{Numerical}$ [g/s]	Difference [%]
1000	1.7	1.2	29
2100	3.8	3.8	0
3000	5.4	6.2	-15

CONCLUSIONS

In the present paper, the lubrication system of a hermetic variable speed compressor used in domestic refrigerators is investigated by means of a finite-volume based, unsteady, laminar, two-phase flow solver (ANSYS-Fluent). In addition, an analytical flow model is developed to obtain the velocity distribution between the rotating crankshaft and the stationary screw pump in Case (A) and the rotating crankshaft with screw flights and the stationary cylindrical apparatus for Case (B) to predict approximate mass flow rates of the lubricant in the compressor. The influence of important physical parameters i.e., the rotational speed of the crankshaft, the oil viscosity, the submersion depth of the crankshaft in the oil sump and as the geometric parameter the effect of the screw aspect ratio (screw helix angle) are investigated both analytically and numerically. It is found that with increasing rotational speed, the mass flow rate increases profoundly. With increasing viscosity and submersion depths, the oil mass flow rates increased very insignificantly both for the numerical and analytical models. It is further observed that increasing the screw aspect ratio also increases the mass flow rate up to a certain limit. In general, analytical flow model overpredicted the oil flow rate for the investigated parameters because the flow domain is larger than the computational domain. Case (B) is more satisfactory in terms of maximizing mass flow rate compared to Case (A) under the same operating conditions because of the screw flights carved on the internal surface of the crankshaft. This study gives further insight into the details of the lubricant's flow characteristics in the lubrication system of the variable speed compressor and reveals some of the important parameter dependencies of the oil mass flow rate. Furthermore the employed analytical model is most useful for pre-design work as it gives much faster prediction based on various parameters.

ACKNOWLEDGEMENTS

The authors are indebted to Ministry of Science, Industry and Technology of Turkey and Arcelik A.S. for financial support through the project 01340-STZ-2012-1.

REFERENCES

Alves M.V.C., Barbosa J.R. Jr., Prata A.T., 2009, "Analytical Solution of Single Screw Extrusion Applicable to Intermediate Values of Screw Channel Aspect Ratio", J. Food Eng., vol. 92 pp. 152-156.

Alves M.V.C., Barbosa J.R. Jr., Prata A.T., 2012, "Analytical and CFD Modelling of the Fluid Flow in an Eccentric-Tube Centrifugal Oil Pump for Hermetic Compressors", International Compressor Engineering Conference, Purdue University

Alves M.V.C., Barbosa J.R. Jr., Prata A.T., 2013, "Analytical and CFD Modelling of the Fluid Flow in an Eccentric-Tube Centrifugal Oil Pump for Hermetic Compressors", Int. J. Refrigeration, vol. 36 pp. 1905-1915.

Alves M.V.C., Barbosa J.R. Jr., Prata A.T., Ribas F.A Jr., 2011, "Fluid Flow in a Screw Pump Oil Supply System for Reciprocating Compressors", Int. J. Refrigeration, vol. 34 pp. 74-83.

ANSYS- Fluent 14.0, 2011, Theory Guide, pp. 500-524.

Kerpicci H., Onbasioglu S.U., Yagci A., Oguz E., 2010, "Numerical Investigation of Oil Flow in a Hermetic Reciprocating Compressor", International Compressor Engineering Conference, Purdue University

Kim H.J., Lee T.J., Kim K.H., Bae Y.J., 2002, "Numerical Simulation of Oil Supply System of Reciprocating Compressor for Household Refrigerators", International Compressor Engineering Conference, Purdue University

Li Y, Hsieh F., 1996, "Modeling of Flow in a Single Screw Extruder", J. of Food Eng., vol.27, pp. 353-375

Lückmann A.J., Alves M.V.C., Barbosa J.R. Jr., 2008, "Analysis of Oil Pumping in a Reciprocating Compressor", International Compressor Engineering Conference, Purdue University.

Lückmann A.J., Alves M.V.C., Barbosa J.R. Jr., 2009, "Analysis of Oil Pumping in a Reciprocating Compressor", Applied Thermal Eng., vol. 29, pp. 3118-3123.

Ozsipahi M., Cadirci S., Gunes H., Sarioglu K., Kerpicci H., 2014, " Numerical Simulation of Lubrication System in a Hermetic Reciprocating Compressor", ASME- Engineering System and Design Analysis (ESDA), Copenhagen.

Ozsipahi M., Cadirci S., Gunes H., Kerpicci H., Sarioglu K., 2014, "A numerical study on the lubrication system for a hermetic reciprocating compressor used in household refrigerators", Int. J. Refrigeration, vol. 48 pp. 210-220.

Tada M. P., Hoffmann T., Couto P.R., Manke A. L., de Bortoli M.G.D., 2014, "Numerical and Experimental Examination for Oil Pump System Using a Simplified Uncoupled Simulation Model", International Compressor Engineering Conference, Purdue University.

Wu W., Li J., Lu L., Feng Q., 2010, "Analysis of Oil Pumping in the Hermetic Reciprocating Compressor for Household Refrigerators", International Compressor Engineering Conference, Purdue University

Mustafa OZSIPAHI has received his bachelor and master's degrees from Mechanical Engineering, Yıldız Technical University in 2011 and Istanbul Technical University in 2014 respectively. Mr. Ozsipahi is currently a research assistant in the Faculty of Mechanical Engineering at Istanbul Technical University. His research area includes numerical investigation of heat and fluid flow problems, specifically the lubrication system of hermetic reciprocating compressors for household applications.

Sertac CADIRCI has received his bachelor degree from Mechanical Engineering, Yıldız Technical University in 2001; master's and Ph.D. degrees from Istanbul Technical University in 2004 and 2010 respectively. Dr. Cadirci is currently an assistant professor in the Faculty of Mechanical Engineering at Istanbul Technical University. His research area includes numerical and experimental investigation of fluid flow problems specifically active flow control applications in laminar boundary layers.

Hasan GUNES has received his bachelor degree from Mechanical Engineering at Istanbul Technical University in 1989. He received his master's and Ph.D. degrees from Mechanical Engineering at Lehigh University in 1993 and 1997 respectively. He is currently a professor in the Faculty of Mechanical Engineering at Istanbul Technical University. He has worked as a researcher in Stuttgart University and Brown University. His research area includes numerical modelling of heat and fluid flow problems, heat transfer, aerodynamics and numerical analysis.

Kemal SARIOGLU has received his bachelor, master's and Ph.D. degrees from Mechanical Engineering, Istanbul Technical University, in 1988, 1990 and 1996 respectively. His research interests lie in the area of turbomachinery, reciprocating compressors, solidification, drying systems and Computational Fluid Dynamics. He worked as an assistant professor at Istanbul Technical University and then as a research specialist at R&D Center of Arcelik A.S., Istanbul, Turkey. Dr. Sarioglu is the best project owner of Koç Holding Group and received awards from the projects he leaded.